EUMETSAT
H SAF
SUPPORT TO OPERATIONAL HYDROLOGY AND WATER MANAGEMENT

A Climate Data Record of Soil moisture in the root zone

EUMETSAT short course

June 16th 2021

David Fairbairn, Patricia de Rosnay

Contents

1. Overview

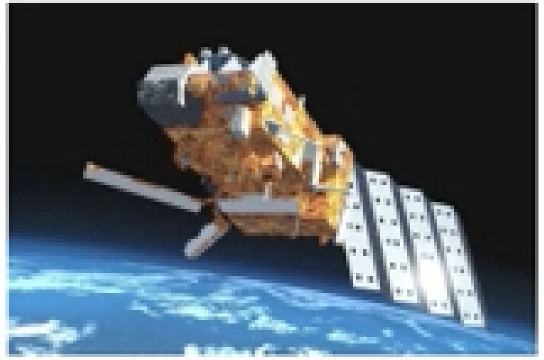

SSM derived from change-detection approach (Wagner et al., 1999)

$\sigma^b = 0.01 m^3/m^3$
$\sigma^{scat} = 0.05 m^3/m^3$

ERA-5 atmospheric forcing

H-TESSEL land surface model

Background errors

Input observations
ERS & ASCAT-A/B
T2m and RH2m

Observation errors

EKF soil moisture analysis

postprocessing

Output root-zone liquid SWI

Simplified Extended Kalman (SEKF) filter of de Rosnay et al., 2013

<u>Simplified EKF analysis</u>

$$\mathbf{x}^a(t_i) = \mathbf{x}^b(t_i) + \mathbf{K}_i\left[\mathbf{y}^o(t_i) - \mathcal{H}_i(\mathbf{x}^b)\right],$$

$$\mathbf{K}_i = \left[\mathbf{B}^{-1} + \mathbf{H}_i^T\mathbf{R}^{-1}\mathbf{H}_i\right]^{-1}\mathbf{H}_i^T\mathbf{R}^{-1},$$

$$\mathbf{H}_{mn,i} = \frac{\mathcal{H}_{m,i}(\mathbf{x}^b + \delta\mathbf{x}_n^b) - \mathcal{H}_{m,i}(\mathbf{x}^b)}{\delta x_n}.$$

SM analysed over first 3 layers in H-TESSEL:
Layer 1: 0-7 cm
Layer 2: 7-28 cm
Layer 3: 28-100 cm
Layer 4 (not analysed): 100-289 cm

- Global root-zone liquid soil wetness index at 10 km sampling
- Assimilates reprocessed scatterometer-derived surface SM and screen-level T2m/RH2m
- Offline surface model forced by ERA5
- Available daily at 00 UTC (H141, 1992-2018) and extended annually (H142, 2019-2020)

2. Advanced Scatterometer (ASCAT) on-board Metop

- Sensor characteristics
  - Active microwave scatterometer
  - Frequency: C-band, 5.255 GHz
  - Polarisation: VV
  - Spatial resolution: 25/50 km
  - Antennas: 2 x 3
  - Swath: 2 x 500 km
  - Multi-incidence: 25-65°
  - Daily global coverage: 82%

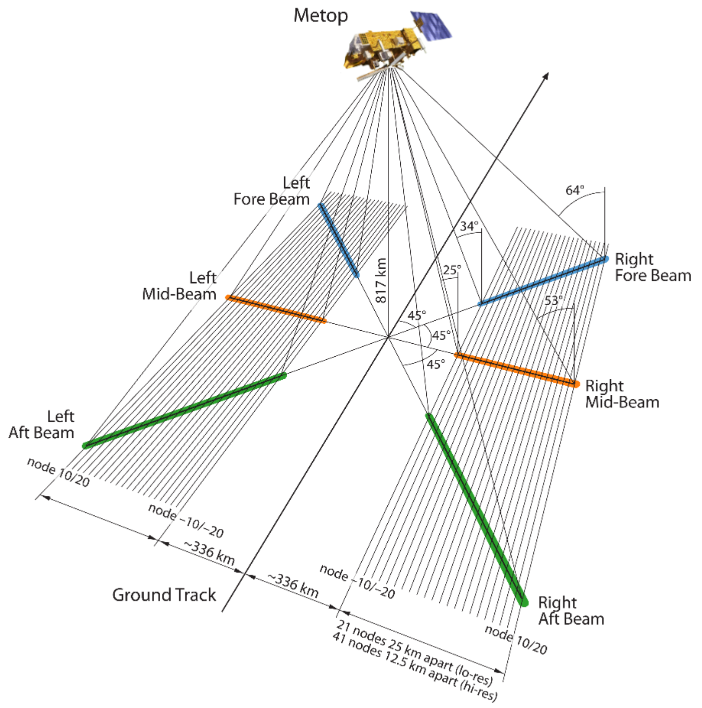

Figa-Saldana, et al., The advanced scatterometer (ASCAT) on the meteorological operational (MetOp) platform: A follow on for European wind scatterometers, Canadian Journal of Remote Sensing, 28(3), 404–412 (2002). http://dx.doi.org/10.5589/m02-035

Spatial coverage in 24 h

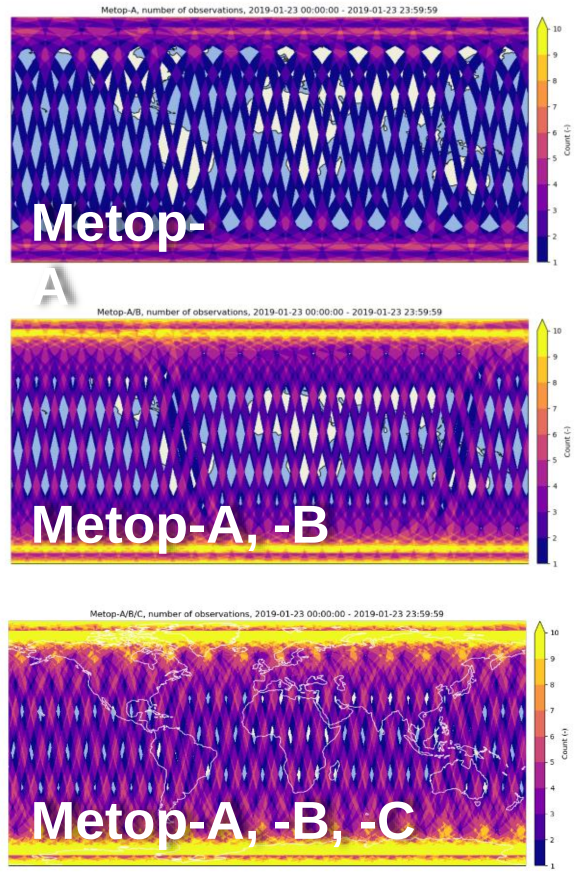

ASCAT observation accuracy

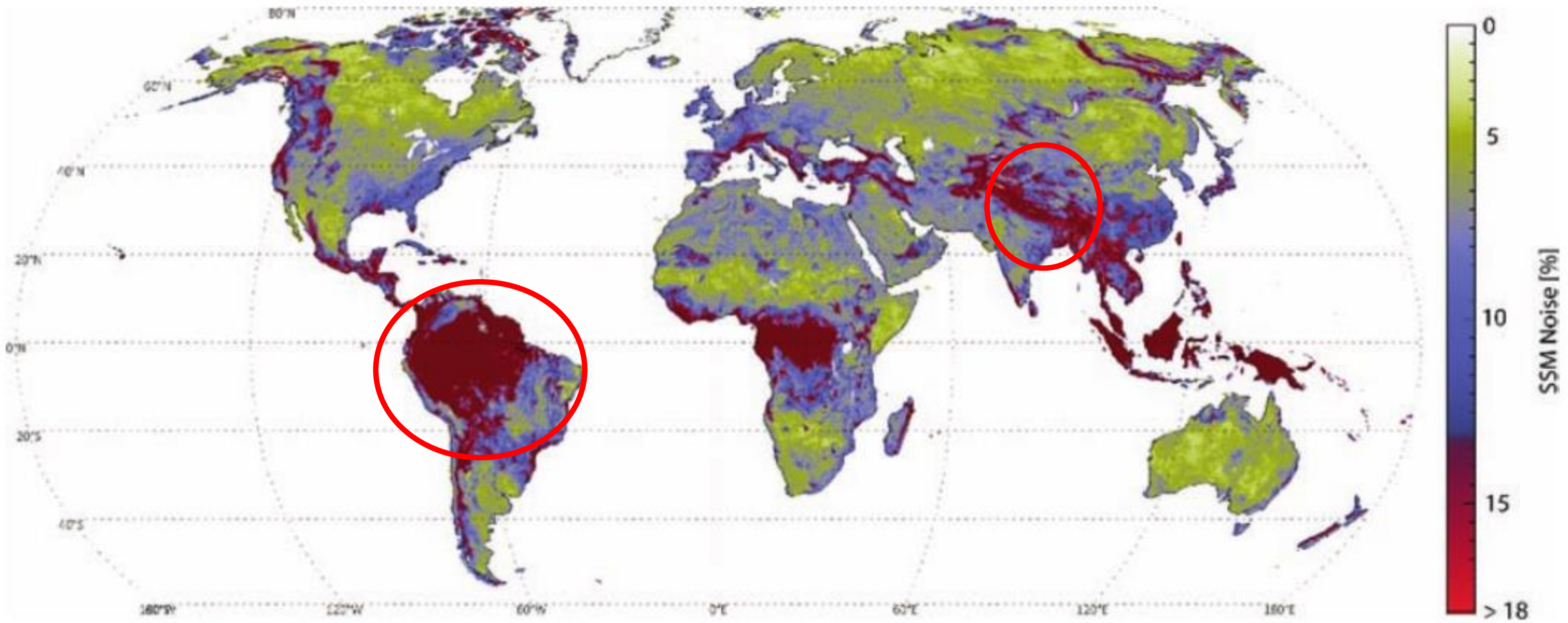

Estimate of noise (%) in ASCAT-derived observations. From Figure 6 of Wagner et al (2013). Based upon the methods presented in Naiemi et al. (2009).

- Most areas have a high signal-to-noise ratio. But observations in highly vegetated regions and mountainous regions are noisy.

3. H-TESSEL land surface model

- Land surface models (LSMs) provide continuous and spatially complete estimates of root-zone soil moisture.

- Dependent on accuracy of model and atmospheric forcing, notably precipitation and radiative forcing;

- LSMs require parameterizations (e.g. soil texture, vegetation type), which are not always accurate;

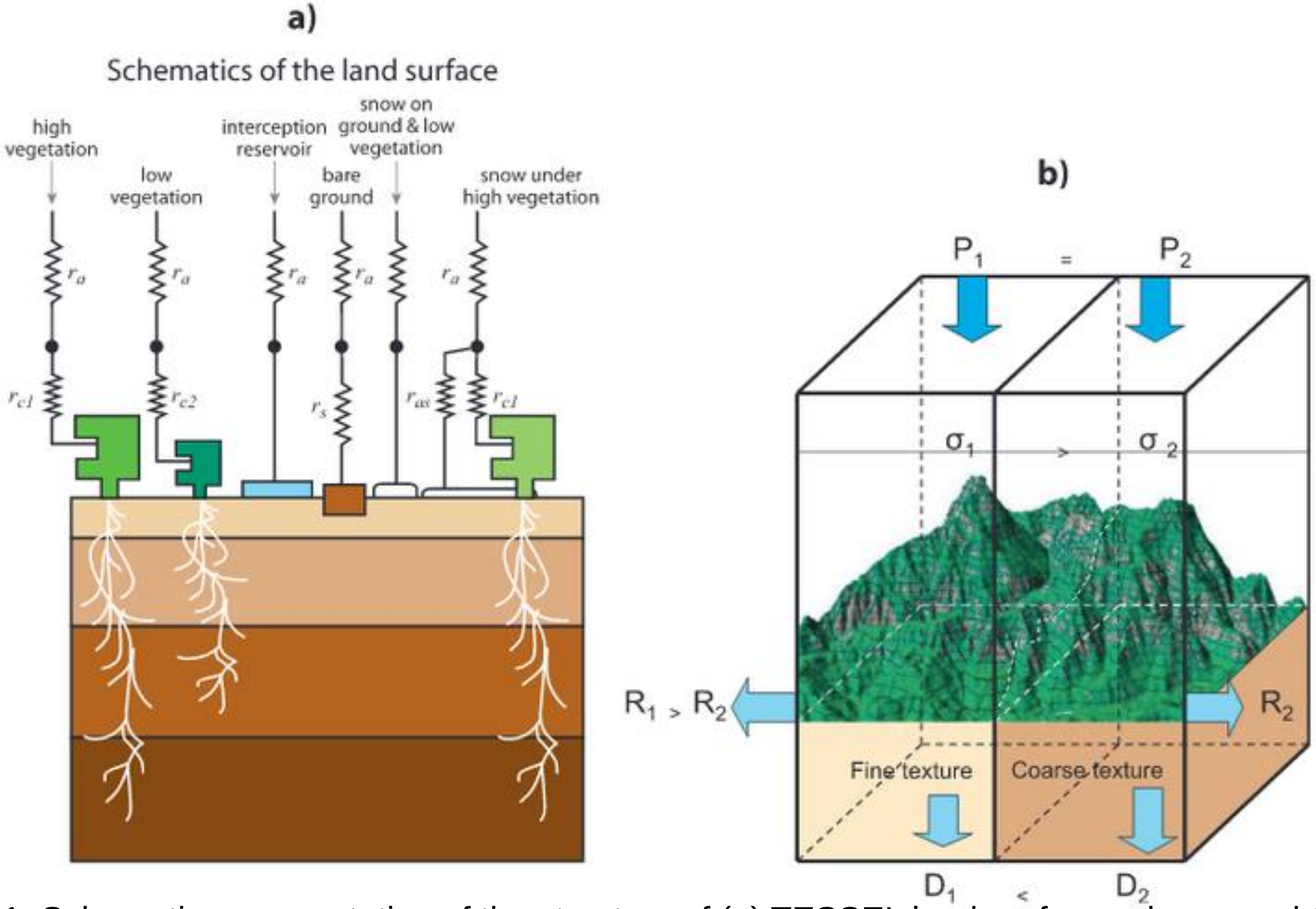

Figure 1: Schematic representation of the structure of (a) TESSEL land-surface scheme and (b) spatial structure added for H-TESSEL. From Balsamo *et al* (2009).

4. CDF matching bias correction

- SEKF method assumes observations are unbiased with respect to model climatology – designed to correct random errors rather than systematic errors;
- Linear CDF matching (Scipal et al., 2008): first two moments of the observation CDF are rescaled to match the model equivalent
  - Slope *B* and intercept *A* calculated from standard deviations and means of model *x* and observations *y* over climatological period (typically 5 years or more):

$$B = \frac{\sigma_x}{\sigma_y}$$

$$A = \bar{x} - B\bar{y},$$

- Rescaled scatterometer observations ($\hat{y}$):

$$\hat{y} = A + B.y$$

- Seasonal CDF matching employed using 3-month moving average (Draper et al., (2009); Barbu et al., (2014))
- By design, CDF matching converts units of ASCAT from soil wetness index to volumetric.

5. SEKF data assimilation

Simplified EKF analysis

$$\mathbf{x}^{\mathrm{a}}(t_i) = \mathbf{x}^{\mathrm{b}}(t_i) + \mathbf{K}_i \left[\mathbf{y}^{\mathrm{o}}(t_i) - \mathcal{H}_i(\mathbf{x}^{\mathrm{b}})\right],$$

$$\mathbf{K}_i = \left[\mathbf{B}^{-1} + \mathbf{H}_i^{\mathrm{T}}\mathbf{R}^{-1}\mathbf{H}_i\right]^{-1} \mathbf{H}_i^{\mathrm{T}}\mathbf{R}^{-1},$$

$$\mathbf{H}_{mn,i} = \frac{\mathcal{H}_{m,i}(\mathbf{x}^{\mathrm{b}} + \delta\mathbf{x}_n^{b}) - \mathcal{H}_{m,i}(\mathbf{x}^{\mathrm{b}})}{\delta x_n}.$$

SM analysed over first 3 layers in H-TESSEL:
Layer 1: 0-7 cm
Layer 2: 7-28 cm
Layer 3: 28-100 cm
Layer 4 (not analysed): 100-289 cm

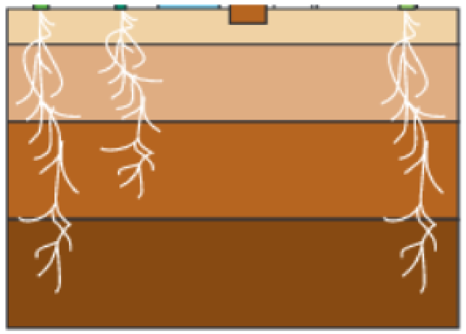

- SEKF based on de Rosnay et al, (2013);
- **B** is diagonal, with background-error standard deviation 0.01 m^3m^{-3} for each layer;
- **R** is diagonal, with observation-error standard deviation 0.05 m^3m^{-3} for ASCAT-derived SSM, 1 K for 2 m temperature and 4% for relative humidity.

SEKF data assimilation

Simplified EKF analysis

$$\mathbf{x}^a(t_i) = \mathbf{x}^b(t_i) + \mathbf{K}_i\left[\mathbf{y}^o(t_i) - \mathcal{H}_i(\mathbf{x}^b)\right],$$

$$\mathbf{K}_i = \left[\mathbf{B}^{-1} + \mathbf{H}_i^T\mathbf{R}^{-1}\mathbf{H}_i\right]^{-1}\mathbf{H}_i^T\mathbf{R}^{-1},$$

$$\mathbf{H}_{mn,i} = \frac{\mathcal{H}_{m,i}(\mathbf{x}^b + \delta\mathbf{x}_n^b) - \mathcal{H}_{m,i}(\mathbf{x}^b)}{\delta x_n}.$$

SM analysed over first 3 layers in H-TESSEL:
Layer 1: 0-7 cm
Layer 2: 7-28 cm
Layer 3: 28-100 cm
Layer 4 (not analysed): 100-289 cm

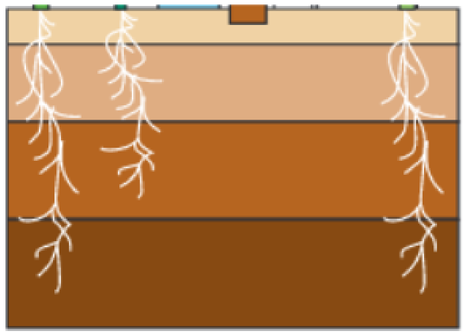

- Jacobian elements H_{mn} for analysis variable n and observation m calculated using finite differences:

SEKF data assimilation

Simplified EKF analysis

$$\mathbf{x}^a(t_i) = \mathbf{x}^b(t_i) + \mathbf{K}_i\left[\mathbf{y}^o(t_i) - \mathcal{H}_i(\mathbf{x}^b)\right],$$

$$\mathbf{K}_i = \left[\mathbf{B}^{-1} + \mathbf{H}_i^T\mathbf{R}^{-1}\mathbf{H}_i\right]^{-1}\mathbf{H}_i^T\mathbf{R}^{-1},$$

$$\mathbf{H}_{mn,i} = \frac{\mathcal{H}_{m,i}(\mathbf{x}^b + \delta\mathbf{x}_n^b) - \mathcal{H}_{m,i}(\mathbf{x}^b)}{\delta x_n}.$$

SM analysed over first 3 layers in H-TESSEL:
Layer 1: 0-7 cm
Layer 2: 7-28 cm
Layer 3: 28-100 cm
Layer 4 (not analysed): 100-289 cm

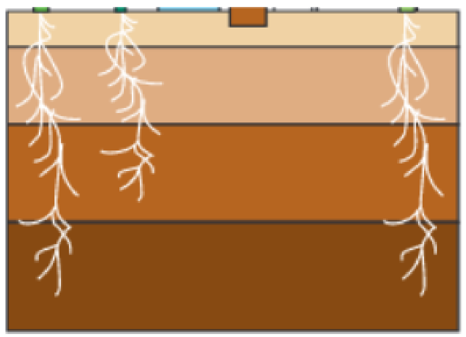

- Jacobian elements H_{nm} for analysis variable n and observation m calculated using finite differences:

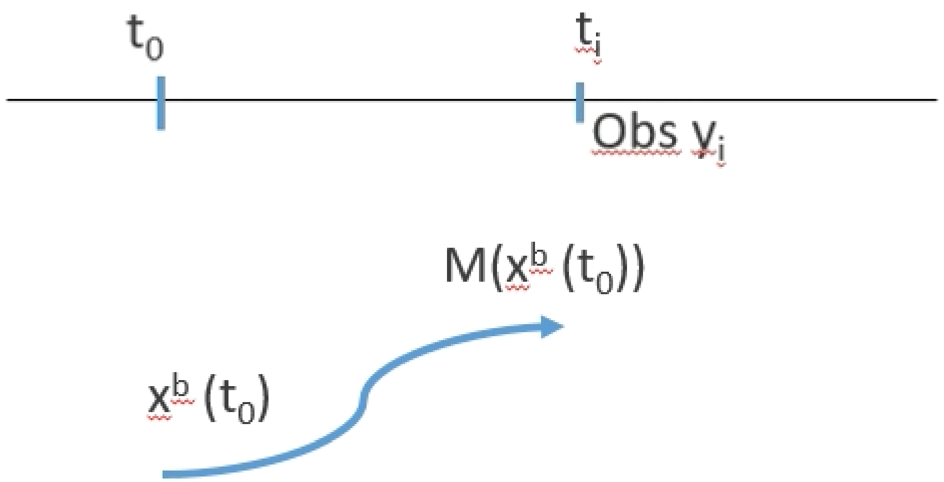

SEKF data assimilation

Simplified EKF analysis

$$\mathbf{x}^a(t_i) = \mathbf{x}^b(t_i) + \mathbf{K}_i\left[\mathbf{y}^o(t_i) - \mathcal{H}_i(\mathbf{x}^b)\right],$$

$$\mathbf{K}_i = \left[\mathbf{B}^{-1} + \mathbf{H}_i^T\mathbf{R}^{-1}\mathbf{H}_i\right]^{-1}\mathbf{H}_i^T\mathbf{R}^{-1},$$

$$\mathbf{H}_{mn,i} = \frac{\mathcal{H}_{m,i}(\mathbf{x}^b + \delta\mathbf{x}_n^b) - \mathcal{H}_{m,i}(\mathbf{x}^b)}{\delta x_n}.$$

SM analysed over first 3 layers in H-TESSEL:
Layer 1: 0-7 cm
Layer 2: 7-28 cm
Layer 3: 28-100 cm
Layer 4 (not analysed): 100-289 cm

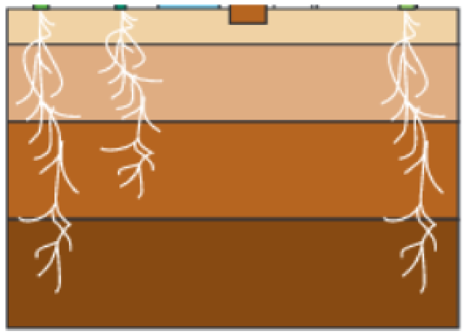

- Jacobian elements H_{nm} for analysis variable n and observation m calculated using finite differences:

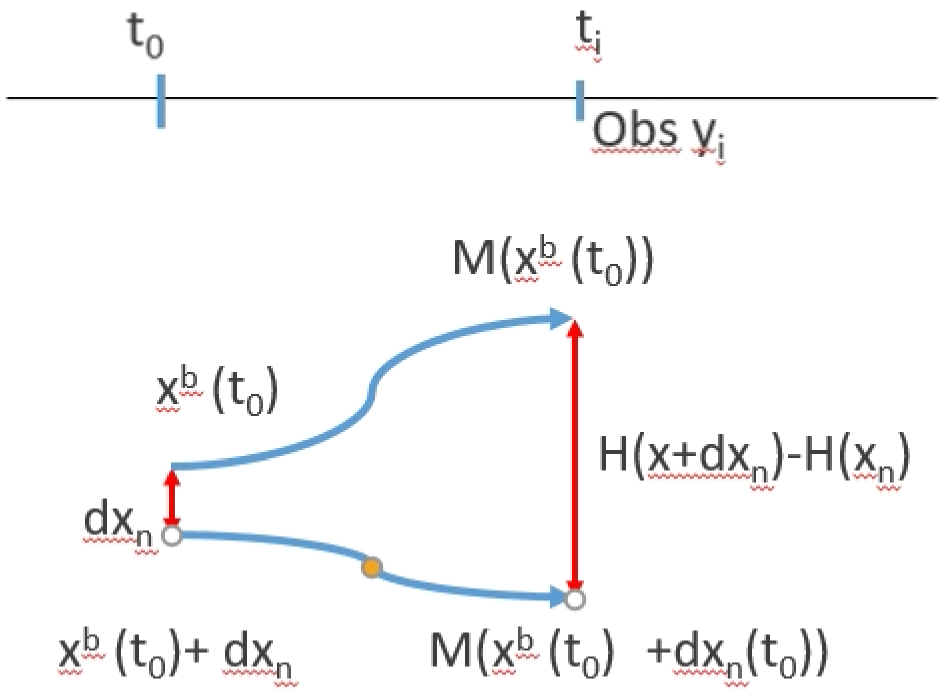

Average daily RZSM increments

January 2009:

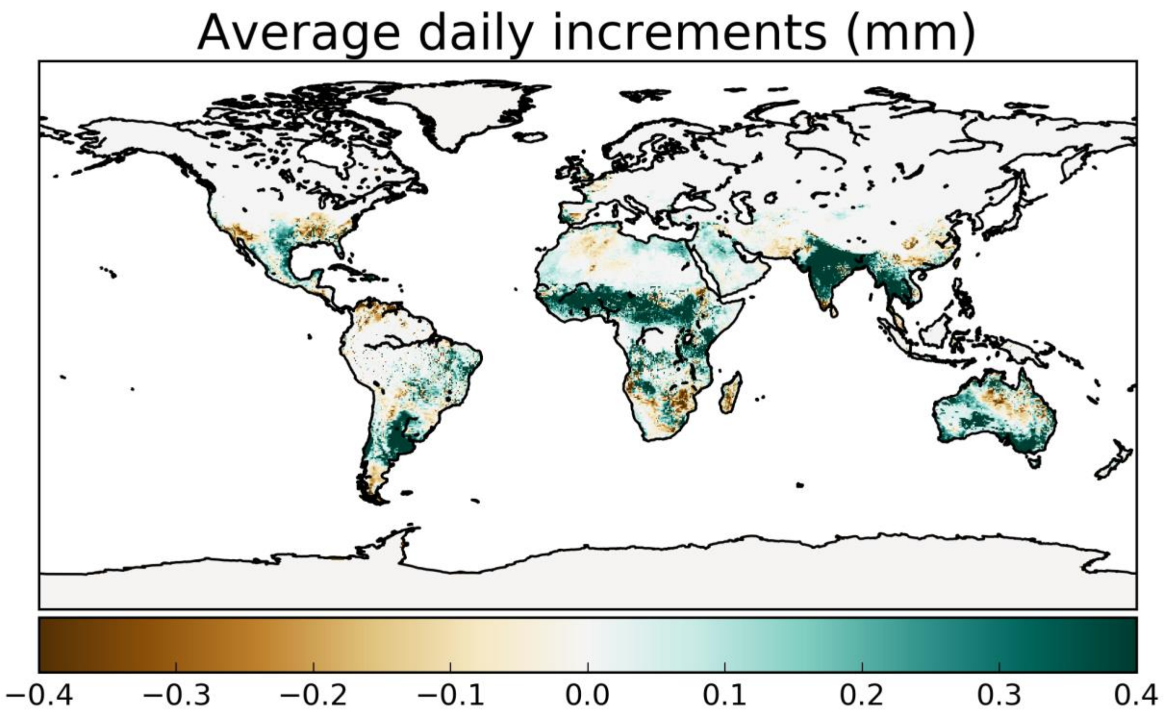

June 2009:

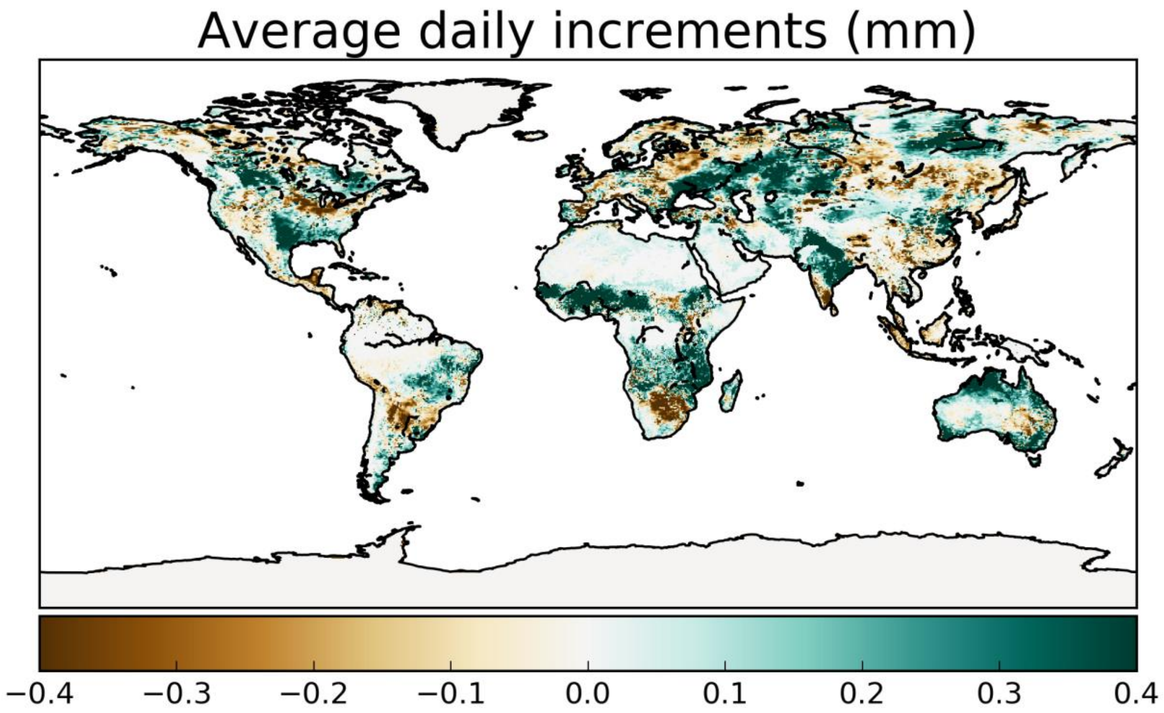

6. Post-processing (volumetric to SWI)

EUMETSAT H SAF
SUPPORT TO OPERATIONAL HYDROLOGY AND WATER MANAGEMENT

Volumetric soil moisture analysis is converted to liquid soil wetness index (SWI):

1. The frozen fraction follows a linear relationship with temperature between -3 ◦ C and 1 ◦ C:

$$F = \frac{1 - ST}{4}$$

2. Only water below field capacity (SM_{cap}) can be frozen.
   - Below field capacity, $SM_{liq} = (1 - F) * SM$
   - Above the field capacity, $SM_{liq} = SM - (F * SMcap)$
3. Conversion of liquid volumetric SM to SWI (divide by saturated value):

$$SWI = \frac{SM_{liq}}{SM_{sat}}$$

7. Data record validation

EUMETSAT H SAF
SUPPORT TO OPERATIONAL HYDROLOGY AND WATER

- RZSM validated annually with in situ data from networks in four countries:
(1) SMOSMANIA (France)
(2) USCRN/SCAN/SNOTEL (US)
(3) REMEDHUS (Spain)

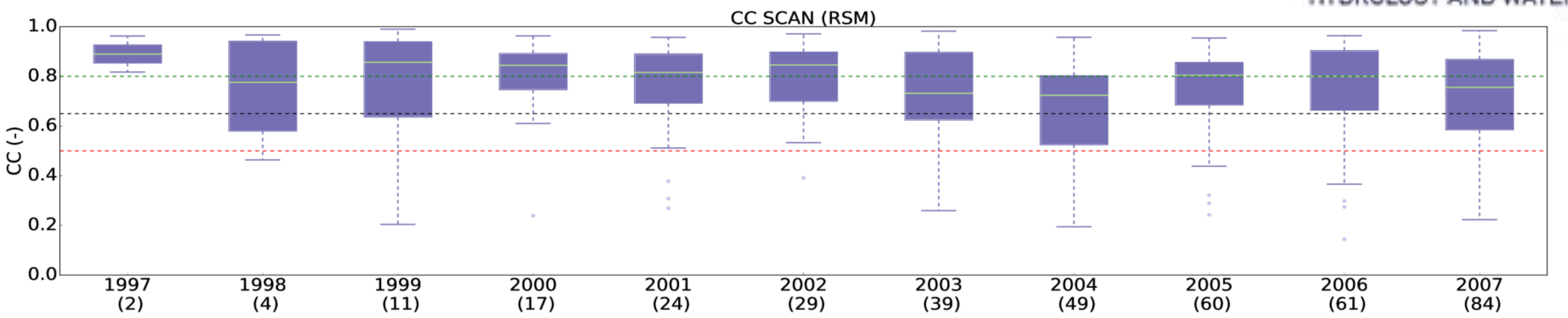

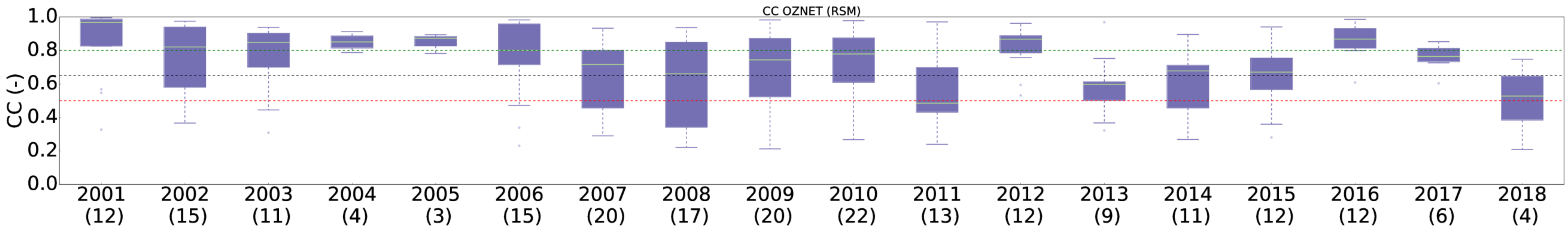

- Good overall performance, with CC>0.65 over most stations

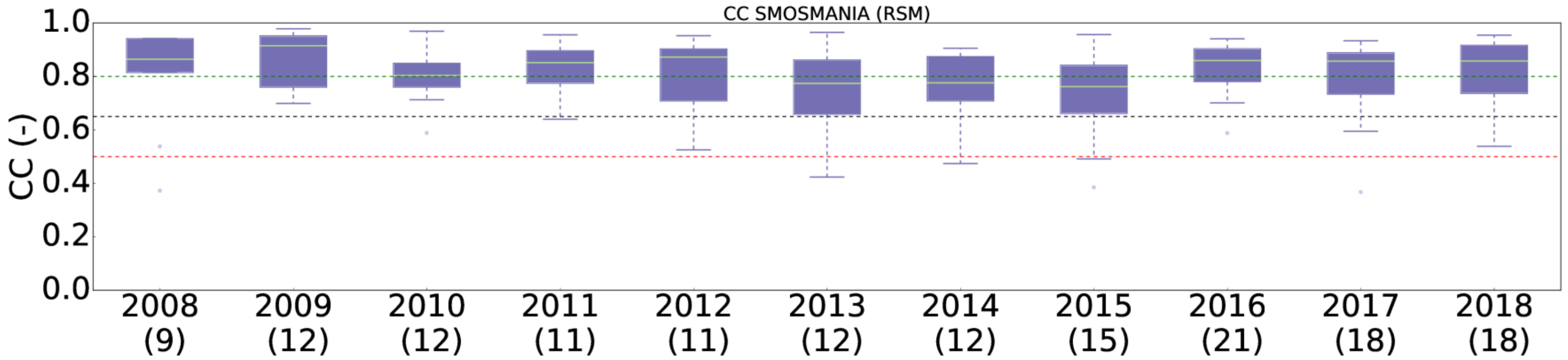

8. Soil moisture trends (1992-2020)

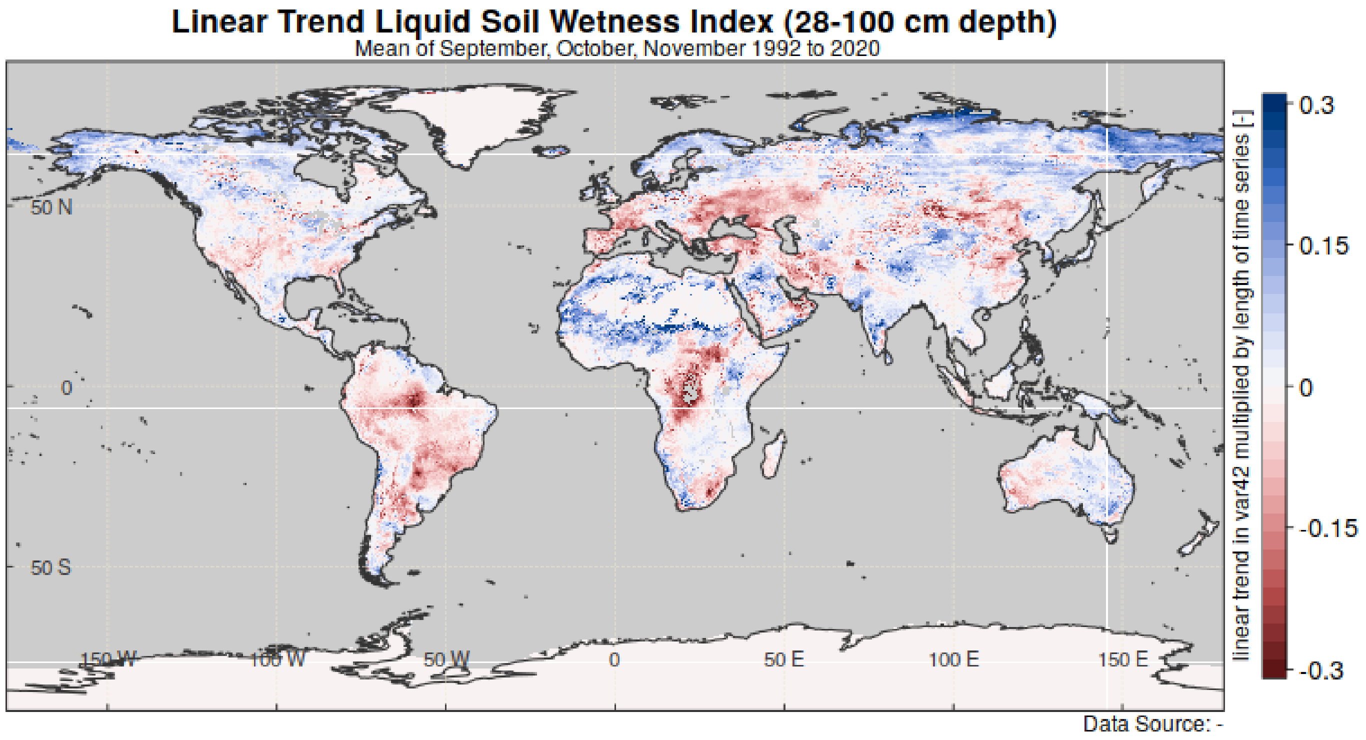

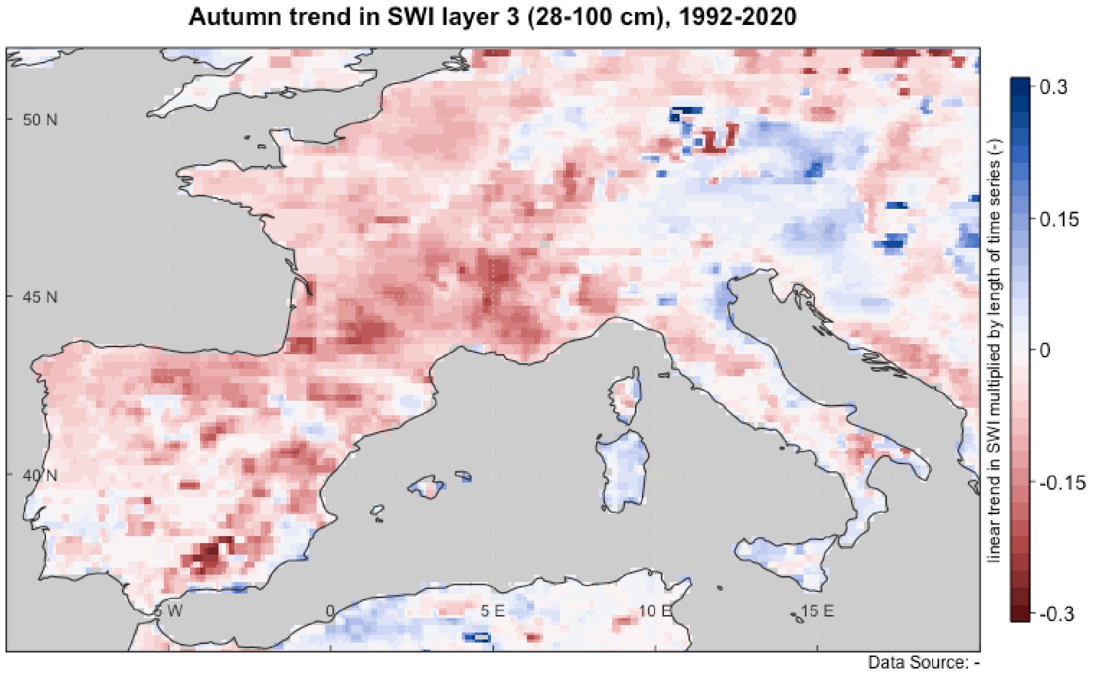

Trends calculated using CMSAF toolbox software (Kothe et al., 2019)

- Soil moisture has decreased by up to 30% in midlatitude autumn months, especially Europe
- Winter/spring trends are less significant
- Possible climate change mechanisms:

(1) Hotter summers drying soil

(2) Relative humidity reducing due to land warming faster than sea (Simmons *et al.*, 2010)

Recent Soil moisture anomalies

EUMETSAT H SAF
SUPPORT TO OPERATIONAL HYDROLOGY AND WATER MANAGEMENT

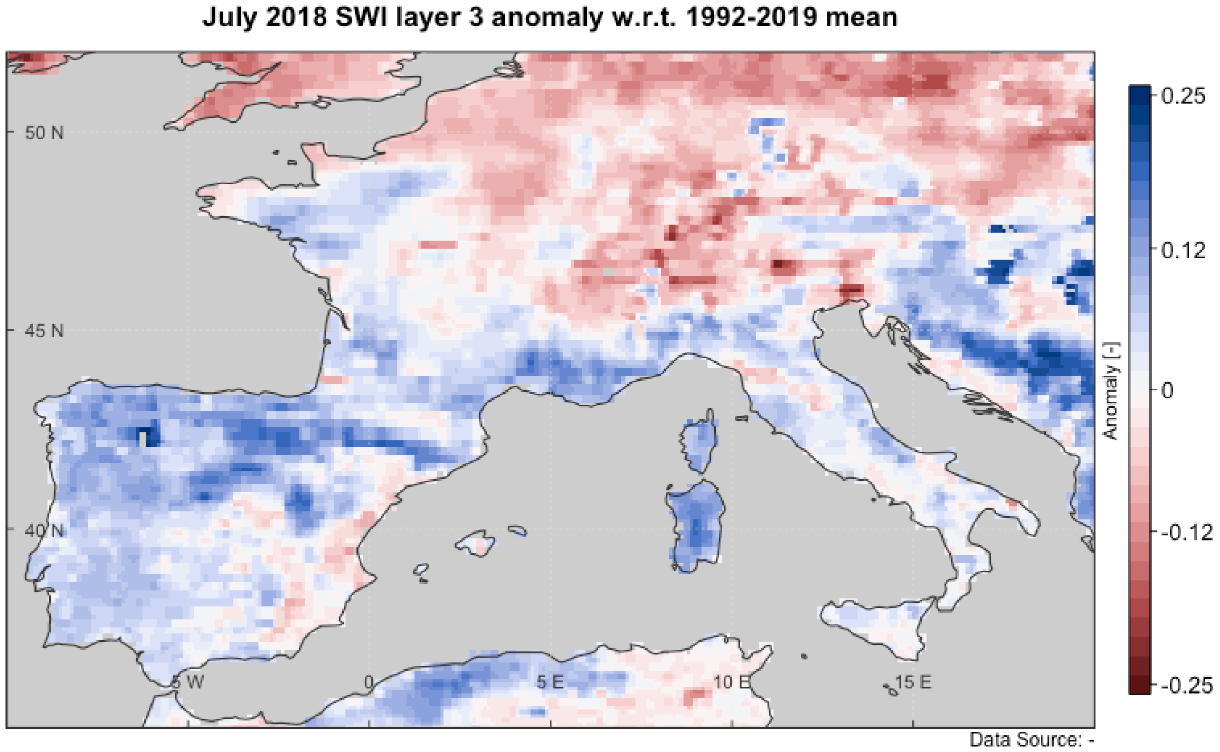

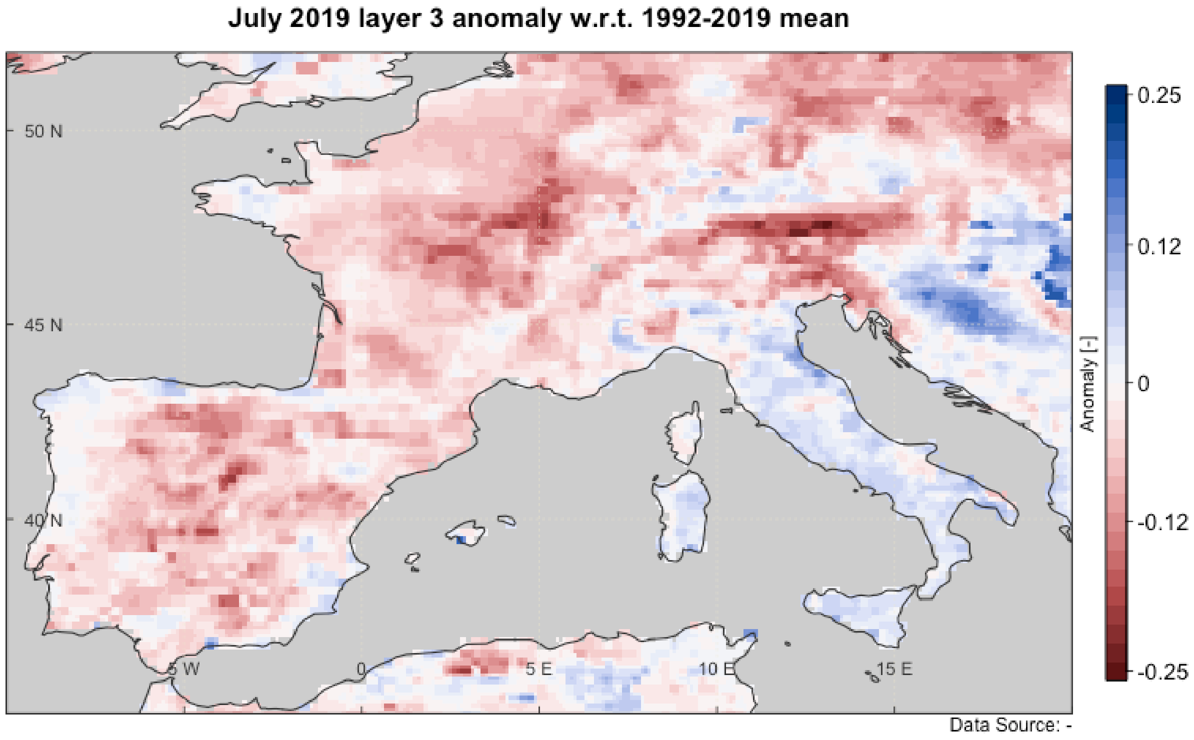

Anomalies calculated using CMSAF toolbox software (Kothe et al., 2019)

- Contrasting soil moisture conditions in July 2018 associated with dry (wet) weather over northern (southern) Europe
- Widespread dry conditions over July 2019 over Europe, when several temperature records were broken
- Recent dry conditions slightly amplified trends in previous slide

Summary

- Global H SAF root-zone soil wetness index data record (H141, 1992-2018) and Offline extension (H142, 2019-2021) at 10 km sampling
- Scatterometer-derived SSM and SLV data assimilation in offline LDAS forced by ERA5
- Bias correction of scatterometer-derived SSM performed using CDF matching
- SEKF data assimilation provides dynamic link between assimilated obs and soil moisture layers
- Post-processing converts volumetric soil moisture analysis to liquid SWI
- Data record well correlated with in situ data (US, France and Spain) with average CC>0.65
- Drying of root-zone SM over Europe (1992-2020) in summer/autumn probably linked to hotter summers and a reduction in relative humidity

Future work

- In 2023, new RZSM data record to be released (H145,1992-2022) with
  - recalibrated scatterometer bias correction
  - 12-hour assimilation windows (consistent with near-real-time H26 product).
  - Dynamic SEKF Jacobians from ensemble of data assimilations (EDA)

- EUMETSAT 2nd generation (EPS-SG) scatterometer derived surface soil moisture data to be assimilated in future data records – higher spatial resolution (12.5 km) than current ASCAT (25 km)

User information

- **To access H SAF data**, first register with H SAF: http://hsaf.meteoam.it/user-registration.php to obtain username and password

- **User documentation/training:**
  - PUM, ATBD and validation reports for H141/H142: https://confluence.ecmwf.int/display/LDAS/H+SAF
  - Online user training course: http://hsaf.meteoam.it/training-courses.php
  - EUMETRAIN event week 4th – 8th November 2019: http://eumetrain.org

References

Barbu, A.L., Calvet, J.C., Mahfouf, J.F. and Lafont, S., 2014. Integrating ASCAT surface soil moisture and GEOV1 leaf area index into the SURFEX modelling platform: a land data assimilation application over France. Hydrology and Earth System Sciences, 18(1), p.173.

De Rosnay, P., Drusch, M., Vasiljevic, D., Balsamo, G., Albergel, C. and Isaksen, L., 2013. A simplified Extended Kalman Filter for the global operational soil moisture analysis at ECMWF. Quarterly Journal of the Royal Meteorological Society, 139(674), pp.1199-1213.

Draper, C.S., Mahfouf, J.F. and Walker, J.P., 2009. An EKF assimilation of AMSR-E soil moisture into the ISBA land surface scheme. Journal of Geophysical Research: Atmospheres, 114(D20).

H SAF (2020): Scatterometer Root Zone Soil Moisture (RZSM) Data Record 10km resolution - Multimission, EUMETSAT SAF on Support to Operational Hydrology and Water Management, DOI: 10.15770/EUM_SAF_H_0008. http://doi.org/10.15770/EUM_SAF_H_0008

Kothe, S., Hollmann, R., Pfeifroth, U., Träger-Chatterjee, C. and Trentmann, J., 2019. The CM SAF R Toolbox—a tool for the easy usage of satellite-based climate data in NetCDF format. ISPRS International Journal of Geo-Information, 8(3), p.109.

Scipal, K., Drusch, M. and Wagner, W., 2008. Assimilation of a ERS scatterometer derived soil moisture index in the ECMWF numerical weather prediction system. Advances in water resources, 31(8), pp.1101-1112.

Simmons, A.J., Willett, K.M., Jones, P.D., Thorne, P.W. and Dee, D.P., 2010. Low-frequency variations in surface atmospheric humidity, temperature, and precipitation: Inferences from reanalyses and monthly gridded observational data sets. Journal of Geophysical Research: Atmospheres, 115(D1).